

SFSA Cast in Steel 2025- George Washington's Sword

Technical Report

Colorado School of Mines- A Washing-Ton of Steel



Colorado School of Mines Team Members:

Samuel Nikolai, Graham Garlitos, Zachary Plummer, Wesley Montgomery

Colorado School of Mines Faculty Advisor:

Sarah Harling, Hot Shop Supervisor and Foundry Educational Foundation Professor

Colorado School of Mines Industry Sponsors:

Western Foundries

Executive Summary

The Colorado School of Mines cuttöe sword for the 2025 SFSA Cast in Steel Competition shows the design, casting, and post-processing of a historically inspired cuttöe that meets George Washington's known preferences. It also demonstrated the capabilities of modern casting techniques. A AISI 4140 sand cast steel component was manufactured using 3D printed molds and investment casting for high detail decorative elements. All manufacturing took place at Colorado School of Mines. Post-cast processing, including forging, normalizing, austenitizing and quenching, and tempering, significantly increased the mechanical properties and microstructure of the submission. Although silicon segregation led to poor feeding and the resulting porosity, the post-processing and testing showed to have mostly negated these detrimental effects. Despite the challenges, the submission highlighted potential of modern casting technologies and can withstand the rigorous testing requirements, which is validated by mechanical testing.

Introduction

In recent years, advances in metal casting technologies such as 3D printing, fluid flow and solidification modeling, and improved melt quality practices have expanded the capabilities of the casting process, allowing for higher performance steel components with intricate designs. SFSA has created the Cast in Steel competition to encourage students to learn about making steel products using the casting process and applying the latest technology available. The 2025 competition challenges teams to produce a cast replica of one of George Washington's swords or to design one based on his known preferences and needs.

George Washington is a legendary figure in America's history, renowned for his leadership in the French and Indian War, Revolutionary War, and as the first President. Washington carried a variety of swords throughout his military career, with multiple styles befitting his station. Erik Goldstein states that there is no doubt that Washington had a sword every time his uniform was on and appeared at the head of his command. However, he also states that it "would be a mistake to imagine Washington brandishing his sword like a brigand and slicing his way through a line of hapless redcoats." As a gentleman and commander, Washington was aware of the etiquette of a sword. In his will, Washington stated "These swords are accompanied with an injunction not to unsheathe them for the purpose of shedding blood, except it be for self-defense, or in defense of their Country and its rights; and in the latter case, to keep them unsheathed, and prefer falling with them in their hands, to the relinquishment thereof."

Erik Goldstein also comments on Washington's sword preferences, stating that the Alte Presentation Sword is likely his least favorite; it arrived in an irregular fashion with a request for money, in addition to "being a poorly balanced cavalry sword, oozing with embellishment, of the type Washington would have no use for. The etchings of the blade, although beautiful and well done, are overcomplimentary and seem like the sort of thing he would not have cared for; much like he was opposed to his portrait appearing on the circulating American coins of the period." Goldstein goes on to state that the Bailey cuttöe was Washington's favorite. From this information it can be concluded that Washington desired a beautiful, simplistic sword that can be both ornamental and practical. This assessment can be corroborated by Jeffrey H. Schwartz,

who stated “First, regardless of his down to earth persona, Washington was still of English aristocratic background.”

A cuttöe sword was manufactured based on Washington’s needs and preferences for the competition; several of Washington’s swords were cuttöes and fit his needs well. “Cuttöe” refers to a curved blade and comes from the French term *couteaux de chasse*, which means hunting knife. Another term to describe this type of sword would be hanger blade. Cuttöes are typically shorter than smallswords and designed for hunting, but also highly utilized by British military officers due to its shape and size favoring hunting and close-quarters combat. Due to the status of the officers and aristocrats wielding this type of sword, it is typically adorned with an ornamental handle, knuckle chain or guard, and silver pommel, often in the design of a lion. The blade of a cuttöe is curved and designed for chopping and slicing, with some thrusting ability. It has a curve that assists in the act of slashing, while the point is not offset enough from the handle to impede thrusting. In terms of warfare at this time a slash can incapacitate an opponent but may not cut through heavy wool jackets or armor; conversely, a thrust could puncture an opponent’s heavy jacket or armor. The cuttöe is also relatively short and lightweight, allowing for quick strikes and slices, parrying, and defensive maneuvers. These characteristics made it a good sidearm at this time for an officer on the battlefield. Officers carried the cuttöe as a sidearm for close quarters fighting rather than a primary weapon and as a symbol of rank and authority.

Sword Design

The design requirements for the 2025 Cast in Steel competition for George Washington’s sword for the Colorado School of Mines submission include:

- A sword of no more than 2 kilograms (4.4 pounds)
- A sword of no longer than 1.09 meters (43 inches)
- An original sword that would be in the style and appropriate for George Washington that is more than 25 inches long overall with at least 20 inches of blade length and less than 43 inches overall with a maximum blade length of 35 inches.

As designed, the blade meets the specifications with:

- An estimated weight of 1.37 kilograms (3.02 pounds)
- An overall length of 0.953 meters (37.53 inches)
- A blade length of 0.731 meters (28.78 inches)

Additionally, the following design requirements have been set by the team to enhance the appearance and performance of the submission:

- Incorporate the experience and imagery of Colorado School of Mines while still manufacturing an authentic George Washington sword.
- Utilize modern casting technology such as 3D printed molds.
- Showcase the complex geometries casting is capable of through the manufacture of an integrated guard.
- Showcase multiple casting methods for the manufacture of the sword.

The initial design idea was determined by researching common designs for sabers and sidearms for officers during the period, historical examples of swords owned by Washington, and Washington’s use case for each and preferences on functionality and artistic design

elements. It was decided a sword based on Washington's preferences and historical accuracy, but with a unique artistic take would be built on to create the final design. After looking at each of Washington's swords and how effectively each would lend to the casting process, the Lion Headed Cuttoe was chosen as the main inspiration. An iterative approach was used to find sword geometry and features to build off. Sketches and subsequent SolidWorks mockups were made to narrow down the blade design, with the primary designs being either a blade with integrated handguard or separate handguard. The final design idea that was chosen to move forward was a curved blade with integrated handguard, and a handguard and pommel that reflect the Colorado School of Mines in a subdued manner that reflected Washington's aversion to over-embellishment.

Historically, the Sword follows the both the design of the time and Washingtons preference, especially about overly embellished details. The handguard and the pommel were the main areas where decoration was added. The Pommel was based on the Lion-Headed Cuttoe, which symbolizes strength, courage, and protection. Instead of a lion's head, a personalized take was done by making the pommel a brass cast of Blaster the Miniature Burro, who serves as an enduring symbol of the determination and work ethic of all Orediggers. While silver was the traditional pommel material at the time, it was out of budget and brass was used to bring cost down while still creating a beautiful, decorative pommel. The pommel was investment cast to achieve an excellent surface finish and high tolerance for the design. The CAD file was drawn by the Colorado School of Mines Additive in Steel team, and 3D printed out of PLA for the investment cast.

Handguard is also symbolic, elegantly representing the longstanding heritage of the Colorado School of Mines while maintaining functionality. This as well is a sentiment Washington would likely agree with, and the decoration without going overboard matches his preferences as well. An integrated handguard in the shape of a Reuleaux triangle, the shape of the Colorado School of Mines legacy triangle, was chosen. It serves the primary purpose of protecting the user's hand from strikes that travel down the blade. Handguards on the swords used by Washington also served a decorative purpose; engraving and visually interesting shapes are almost always present. As the handguard was to be cast as part of the sword itself, the geometry possible was limited, hence why a Reuleaux triangle was chosen as it was more likely to cast well than thinner shapes seen in several of Washingtons sabers. The large, sloping fillets present at the transition from the sword to the handguard serve two main purposes. For casting, they create less turbulent flow between the thin sword section and large handguard section. From a strength perspective, they eliminate what is typically a major stress concentration and reduce the probability of the sword fracturing at the transition area.

The blade geometry is also accurate, and results in a functional sidearm officers of the time could rely on in close quarters combat. The previously mentioned subtle embellishment lends to a sword that, while functional when an officer needed it to be, served an additional purpose of displaying the status of their rank.

FEA was used to check for stress concentrations in a static study (Fig. 1). Model geometry was simplified to allow for an h-adaptive mesh convergence study to be run within the limits of the SolidWorks Simulation package and available hardware (Fig. 2) and reduce singularity issues. Many small fillets otherwise present were increased in size, and the pommel connection area was removed for the sake of the study due to the presence of fillets below 0.1" in radius and the fact that it was not a primary point of interest when looking potential failure points on the sword. A 300 N load was applied to the top curve, and the tang was constrained using roller fixities in the X, Y, and Z direction. The tang-handguard and blade-handguard transitions showed low stress, far from the yield stress of the material. The maximum Von-Mises stress of 131900 psi was located at the bottom of the primary bevel, at the tip of the blade.

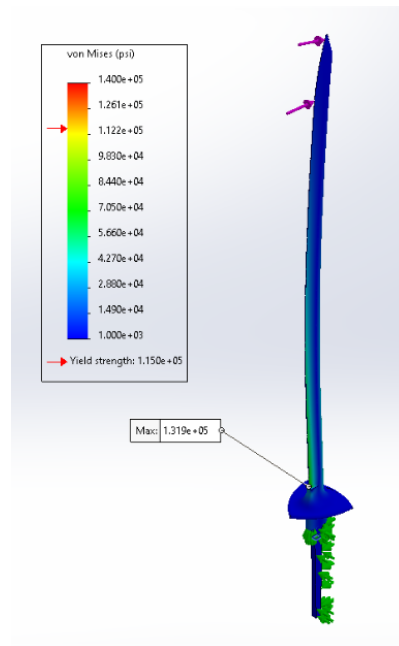


Figure 1: Static Study of Top Strike

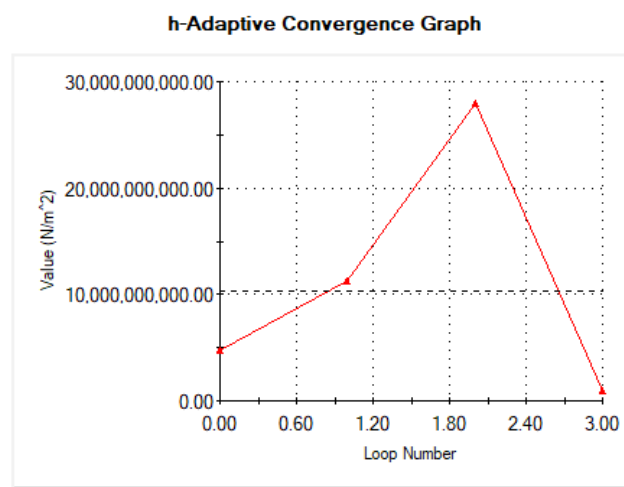


Figure 2: h-Adaptive mesh convergence study

Similarly, handles were traditionally ivory during this time period. Ivory was likewise outside the budget, so buffalo horn was substituted. Bison horn was available during the time period these swords were made, as showcased by Figure 3. This could have been used for sword handles during this time, which is another reason it was selected.

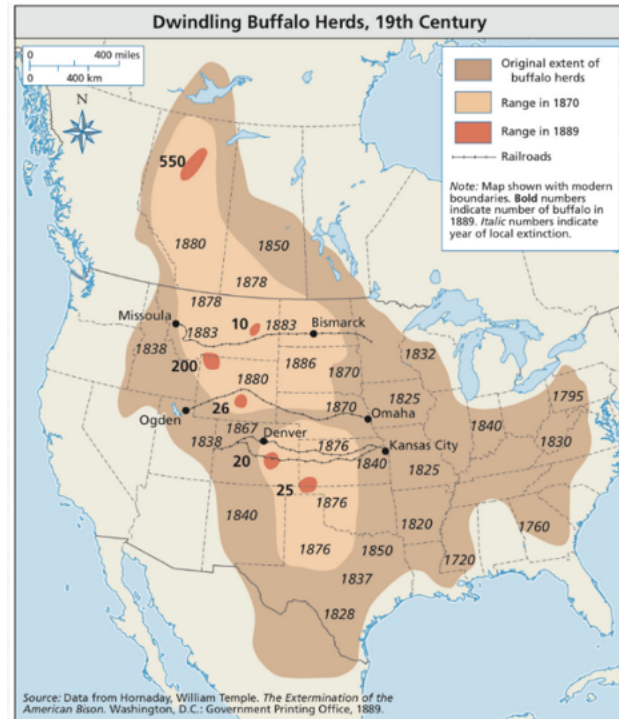


Figure 3: Buffalo Population Range Over Time

The cuttose was cast in a sand mold to improve the quality of the submission. Although an investment mold would result in a better surface finish and higher tolerance of the cuttose, it is more expensive and the Colorado School of Mines foundry lacks the ability to burn out an investment mold of the size of the sword. Additionally, facilities nearby such as Art Castings of Colorado require a pure wax pattern to burn out, which is not within the capabilities at this time as PLA 3D prints have been primarily used for patterns in the past. Colorado School of Mines has attempted to overcome this limitation with a 3D printed wax pattern in the past courtesy of 3D Systems, however, the wax pattern was too fragile and broke during transportation. A sand mold was selected for a number of reasons, first and foremost that it allowed the best chance of success. Sand molds are much cheaper to manufacture and due to a prior relationship with Matthews Additive Technology 3 3D printed sand molds were able to be produced. In past submissions, the molds have been made of silica sand with the gating and risering hand carved. Utilizing a 3D printed mold allowed for much more complex gating and riser designs as well as improved quality of the mold compared to past submissions.

Figure 4 show the final pattern. Campbell's 10 Rules of casting were reviewed and utilized for the design of the mold. For the sprue system a conical pour cup was utilized to reduce spills, as the steel was poured at the Colorado School of Mines facility and technologies such as molding machines and shrouds were not available as a result. The sprue is conical as the flow of liquid steel will thin as the velocity of the melt increases; using a conical sprue reduces the risk of air entrainment while casting. A basin is seen at the base of the sprue, as the first metal to enter the mold is typically the most turbulent and lowest quality.

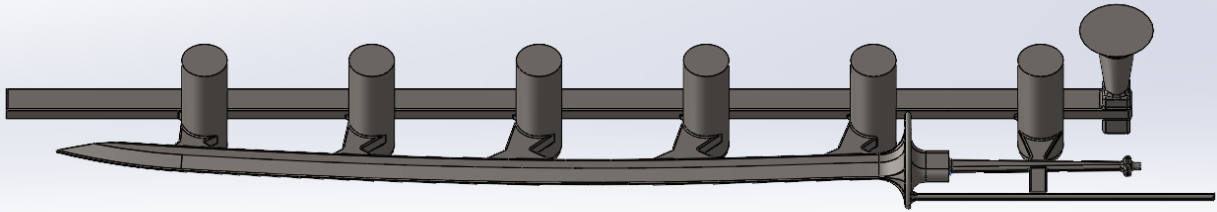


Figure 4: Final Pattern Design

Upon exit from the sprue the metal will enter the runner of the gating system. The runner was designed past the final gate for several reasons; this reduces the risk of turbulent melt entering the cavity first as well as ensuring that filling of the cavity occurs equally across all gates; the melt will flow through the runner, then backfill into the gates once the runner has been completely filled. This again reduces turbulence and allows for all gates to begin filling at the same time.

The gates bisect the risers to aid in solidification and reduce the amount of post-processing that needed to be done. The gates were placed with a slight ledge on the runner to allow the runner to be as close to full as possible before the cavity begins filling and is oriented so metal flows into the casting from numerous points, ensuring proper filling.

The risers were placed on top of the gates to allow for the risers to be cut off along with the gates, reducing the amount of grinding needed post-casting. The risers at this location also allow for directional solidification, increasing the amount of time they are able to feed the casting. The riser sizes were calculated to ensure there sufficient metal in the riser to feed the shrinkage in the casting. The equation used and calculated volume of the riser can be seen below:

$$V_{max} = V_{riser} \left(\frac{14 - S}{S} \right), \text{ where } S \text{ is the percentage volumetric shrinkage}$$

$$V_{riser} = 6.004 \text{ in}^3$$

The risers are cylindrical in shape to create a high volume to surface area ratio, which according to Chvorinov's Rule, increase the solidification time of the risers and allow them to feed the casting for a longer period of time, reducing the chance for shrinkage defects. Chvorinov's Equation, as well as the calculated values of the volume to surface area ratio for both the sword and risers can be found below. This calculation confirms that risers have a larger

volume to surface area ratio, meaning that the risers will solidify after the sword, maximizing feeding time.

$$t_f = C \left(\frac{V}{A} \right)^2$$

$$\left(\frac{V}{A} \right)_{sword} = 0.15$$

$$\left(\frac{V}{A} \right)_{riser} = 0.52$$

The alloy selected for the cuttue was AISI 4140. 4140 is a medium-carbon, chromium-molybdenum alloy steel known for its high toughness and strength. The exceptional toughness and impact resistance make it well suited for applications where blades are subjected to extreme stress, such as the testing performed during the Cast in Steel Competition. These properties reduce the likelihood of chipping or catastrophic failure, ensuring durability under demanding conditions. Additionally, 4140 offers good hardenability, allowing for a heat treatment process that offers balance between ductility and hardness. However, with a carbon content of 0.40% it does not reach the same level of hardness as traditional high carbon sword steel, resulting in decreased edge retention. Despite this trade-off, 4140 offers superior impact resistance, making it a strategic choice of properties for competition settings, where blade durability must be prioritized over prolonged use and sharpness, as well as reducing the likelihood of failure. Additionally, 4140 has been utilized for multiple Colorado School of Mines submissions, allowing for refinement and enhancement of the melt practice and casting quality, ultimately producing cleaner, stronger steel optimized for the competition.

Formation of the right microstructure is of utmost importance for the application. Figure 5 is a solidification model to predict the microstructure. To interpret Figure 5, the x-axis is the solidification velocity (V), and the y-axis is the thermal gradient (G). The regions outside the bounding black lines delineate the conditions for planar growth where a high thermal gradient and low solidification velocity stabilize the solid-liquid interface, preventing perturbations that could initiate dendritic growth. The regions between the grey and black lines correspond to columnar growth, where the thermal gradient is sufficient to maintain directional growth into the liquid. Within the grey lines, dendritic growth occurs as undercooling increases, leading to the formation of primary and secondary dendrite arms. The blue and green lines indicate the conditions for primary (PDAS) and secondary dendrite arms (SDAS).

The orange curve models the columnar-to-equiaxed transition (CET). Conditions above and to the left of this curve favor equiaxed grain formation due to high solidification velocity and lower thermal gradients, alternatively conditions below and to the right, columnar grains dominate due to insufficient nucleation and directional heat flow. Given that silica sand has a relatively low thermal conductivity, the thermal gradient is lower, increasing the likelihood of equiaxed grain formation by reducing directional solidification effects. Additionally, using additions in the form of inoculants will increase nucleation sites, therefore also increasing the likelihood of equiaxed grains. Niobium, a strong grain refiner, was also added. Niobium will refine grains in the melt, increasing the likelihood of equiaxed grains. Pouring at a higher superheat will also increase the chance of equiaxed grains. A silica sand mold will also aid in this

as silica sand has low thermal conductivity, leading to a slower, more uniform cooling rate. This also increased the likelihood of equiaxed grains.

Equiaxed grains are preferable for a sword as they provide numerous benefits to mechanical properties. First, equiaxed grains are isotropic and have more uniform properties when compared to anisotropic columnar grains; swords need to absorb impact forces and equiaxed grains provide more uniform toughness, reducing the risk of brittle fracture. Additionally, as a cuttue is meant for both slashing and thrusting, isotropic mechanical properties will improve the performance of the sword. Cracks in columnar grains will also propagate easier due to the elongated grains, conversely, equiaxed grains will impede crack growth. During heat treatment equiaxed grains also reduce stress, decreasing the chance of warping, and allow more uniform hardening of the blade.

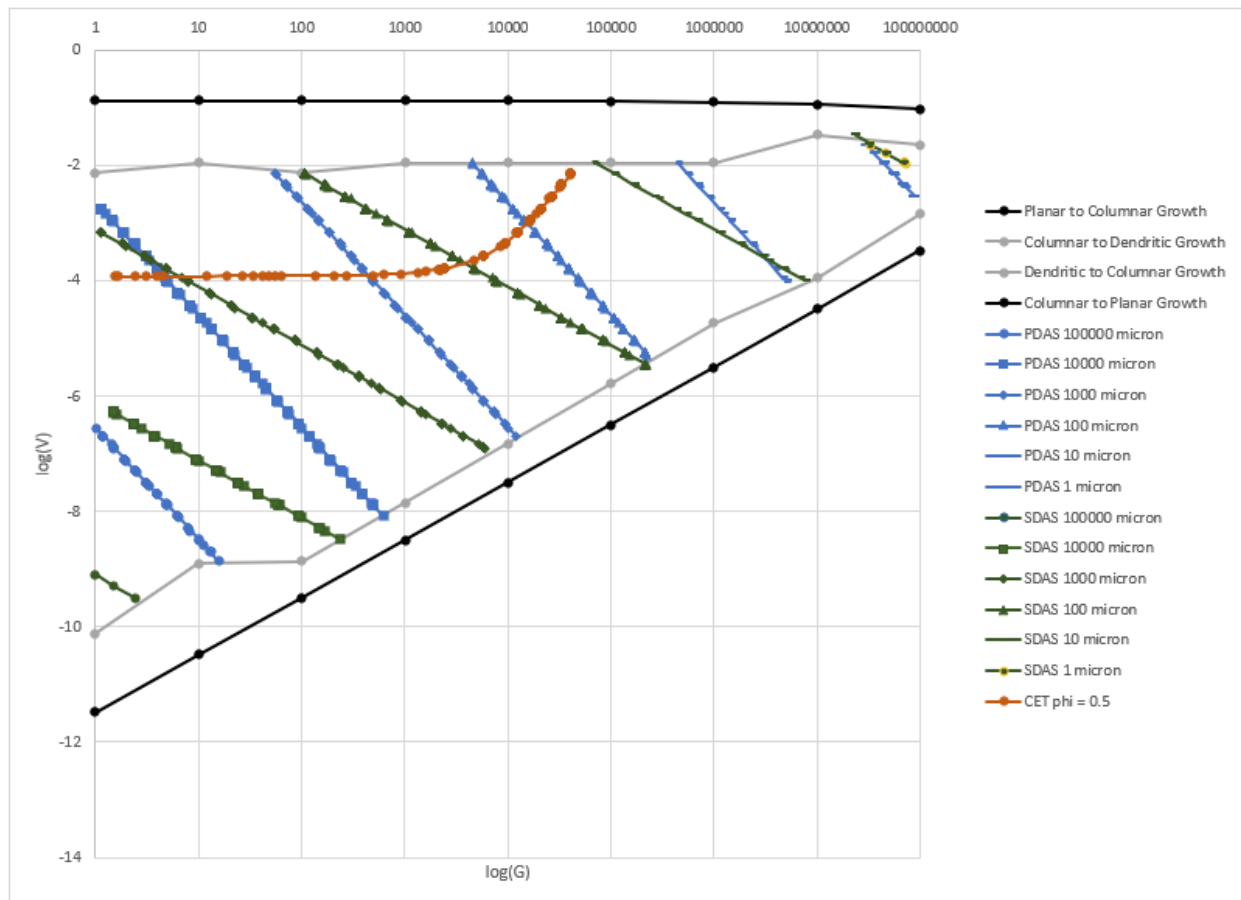


Figure 5: Theoretical solidification model depicting the growth type and transitions, the primary dendrite arm spacing (PDAS), the secondary dendrite arm spacing (SDAS), and the columnar-to-equiaxed transition (CET) models, as characterized by the solidification

Manufacturing:

Sand Casting:

As stated earlier, the sword was sand cast in a 3D printed silica sand mold provided by Matthews Additive Technology from the pattern in Figure 6. Upon arrival of the sand molds, it was evident that the sprue and runner radius was too small and premature freezing in those

parts of the gating system was a risk. As such, the sprue and runner were both drilled out to increase the depth and prevent this effect. Two of the three molds were drilled, while leaving one mold as-received as a control for the steel pour. All three molds were thoroughly vacuumed to ensure no loose sand remained in the cavity, as this loose sand would result in sand inclusions throughout the final casting. Before the molds were closed, they were coated in a silica alcohol slurry; this slurry served as a mold wash as graphite forms a smooth, nonreactive layer on the mold surface to reduce surface roughness. Additionally, it prevents metal penetration into the mold and allows for more uniform cooling due to the high thermal conductivity of graphite. The alcohol was burned out prior to closing the molds. The molds were sealed with Liquid Nails, to reduce the chance of the cope and drag separating during pouring. Steel bands around the mold and mold weights served a similar purpose. Ceramic cups were also added on the top of all the risers and above the sprue as a pour cup to increase the head pressure in the mold and assist with movement of the melt as seen in Figure 7.

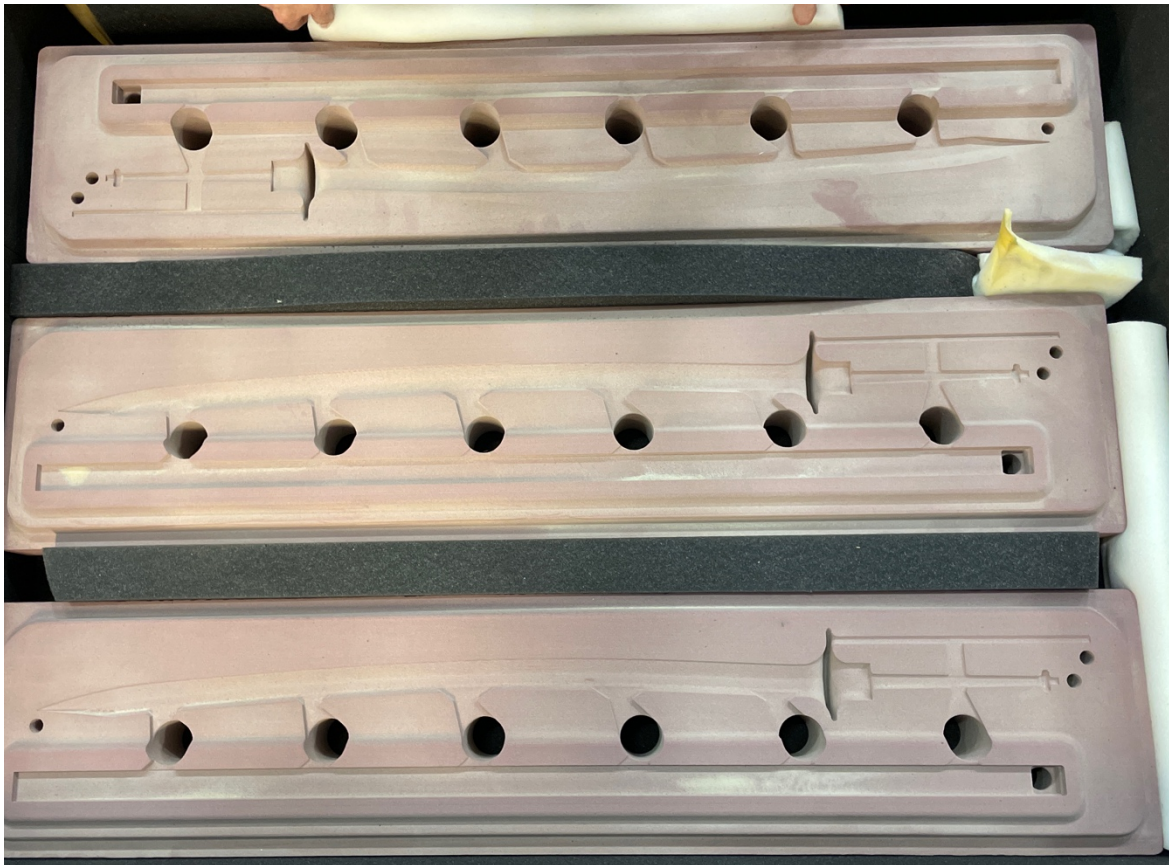


Figure 6: Cope Side of 3D-Printed Molds, Manufactured by Matthews Additive Technologies



Figure 7: Mold Condition Before Pouring

AISI 1045 steel was melted within an induction furnace and alloyed up to the composition of 4140 steel. The composition of the 1045 steel and the target composition of the 4140 steel can be seen below in Tables 1 and 2. 0.75 lbs of ferromanganese, 0.75 lbs of ferromolybdenum, and 3.8 lbs of low carbon chrome were added in the furnace to alloy up to the target composition. Additionally, 0.25 lbs of aluminum shot was added to deoxidize the melt by forming aluminum oxides. 1 lb of 35% ferroniobium was also added to refine the grain size of the casting by forming niobium carbides and niobium nitrides, which restricts grain growth and results in smaller and more uniform grains. Additionally, the strength of the casting will increase due to the formation of carbides and the Hall-Petch effect.

Table 1: Composition of AISI 1045 Charge Material

Element	Fe	C	Cr	Ni	Mo	Si	Mn	Cu	S	P	Al	N	Nb
Composition	98.30%	0.46%	0.05%	0.03%	0.01%	0.23%	0.75%	0.07%	0.02%	0.02%	0.03%	0.03%	0.00%

Table 2: Target Composition for AISI 4140

Element	Fe	C	Cr	Ni	Mo	Si	Mn	Cu	S	P	Al	N	Nb
Composition	97.03%	0.45%	0.95%	0.03%	0.20%	0.21%	0.85%	0.07%	0.02%	0.02%	0.02%	0.03%	0.12%

One heat was used and all 3 of the molds as well as the test bars and plates the charpy samples were machined out of were cast from this heat. The order of pouring was as follows: first sword mold, test bar mold, ingot mold, second sword mold, control sword mold, charpy plate mold, and an additional ingot mold. The temperature of the melt pouring the first mold was 3150°F. All casting was done in the Colorado School of Mines foundry.

Investment Casting:

The Blaster the Burro pommel was investment cast out of CA873 to add a decorative element to the sword and showcase another casting method. CA873 is a silicon bronze, which reduces the viscosity of the melt and allows for better castability. Silicon will allow better fluidity and mold filling and improves the detail of a casting. The pattern of pommel was printed out of PLA with 10% infill, then wax welded to a wax sprue system. 2 patterns were created with each mold having two blaster heads as seen in Figure 8. Following this the mold was started. The mold was created through a series of dips in Ransom and Randolph Suspended Slurry and RancoSil Fused Silica. Two dips were done with fine silica to establish the start of the mold and 5 dips were done with coarse silica. Ransom and Randolph Suspended Slurry is a silica-based, pre-mixed slurry designed for investment casting. Additionally, it has a color indicator to ensure the mold is dry before another dip takes place, ensuring the integrity of the mold. RancoSil Fused Silica is an electrically fused, higher purity silica that has a low thermal conductivity and excellent thermal shock resistance, which makes it an excellent refractory for investment casting. It can be used throughout a shell and the manufacturer promises that this silica will hold dimensions better than competitors and will not hot bulge or deform during casting. The molds were sealed before burnout. The slurry was mixed thoroughly directly before each dip. Unfortunately, due to an inoperable Zahn Gauge no data was available for fluidity of the slurry.

The molds were burned out using a high temperature kiln with heat supplied by a propane tank and burner. The molds remained in the kiln until there was not PLA or wax remaining, measured by the amount of melted wax or PLA exiting the molds. Following burnout, the molds were fired in a separate kiln at 1472°F. The Blaster Head was cast at the Colorado School of Mines Foundry using a gas furnace. No data was taken during the bronze pour due to this being a primarily decorative element. Figure 9 shows the casting after breakout of the ceramic shell.



Figure 8: Investment Molds Prior to Burn-out and Firing



Figure 9: Bronze Investment Casting After Breakout

Post-Cast Processing:

After casting the castings were inspected for defects and quality, so the highest quality sword could be chosen for post-processing. Following this, the gating systems and risers were cut off using an angle grinder and the sword was processed with a wire wheel to remove the majority of the cast scale oxide. During this step a portion was also cut off of the middle of the risers for spark testing to determine the final chemistry of the casting for comparison to the target chemistry and for use in simulations. The sword showcased significant interior porosity so the blade was forged to increase mechanical properties and close porosity inside the blade. Following this initial processing, the blade also went through weld repair to close any remaining surface porosity, as seen in Figure 10. The sword was taken to the Colorado School of Mines Bladesmithing Laboratory for additional processing; the sword was machined to remove the excess material necessary for casting and improve the surface finish to reduce work after heat treatment.



Figure 10: Weld Repair

Three steps were used for heat treating the blade. First, the sword was normalized at 1580°F and air cooled. Normalizing slightly reduces the effect of microsegregation from casting and helps distribute solutes more evenly. Additionally, it will slightly refine the as-cast microstructure and reduce internal stresses within the sword, which will improve mechanical properties and reduces the risk of distortion during quenching. The sword was austenitized at the same temperature for 23 minutes. This temperature and time ensured that the sword is at a uniform temperature and fully in the austenite phase field. The sword will be oil quenched to facilitate a rapid cooling rate to create the conditions for the diffusionless transformation from austenite to martensite. After quenching the sword will be strong, but extremely brittle due to the martensite formation. This is due to a distorted crystal lattice due to supersaturated carbon. The sword was tempered at 370°F for 30 minutes. Tempering caused the trapped carbon to diffuse, forming tempered martensite; tempered martensite is much more stable and ductile than martensite. This will cause the hardness to decrease, while increasing ductility.

Following tempering, the sword was ground to the desired surface finish for aesthetic appeal and to resemble many of Washington's other swords. Once the desired surface finish is present the handle can be attached to the sword. The handle was split in two sides, with the interior machined out to fit the tang. A brass pin was installed in the tang to assist with the integrity and stability of the handle, as use of the sword results in stresses on the handle and pommel. The handle and pommel were bonded to the sword using resin and allowed to dry and seal overnight. Following the attachment of the handle and pommel the secondary bevel of the sword was machined. Before shipping the sword was coated in oil to avoid rusting.

Metallurgy and Quality:

Concurrently with inspection, the melt quality and composition of the sword was confirmed. The chemistry was analyzed using spark testing courtesy of Western Foundry and X-Ray Fluorescence. Tables 4 and 5 show the data for spark testing and X-Ray Fluorescence (XRF). Note that spark testing does not indicate elements that are not typically used in Western Foundries steel, such as Niobium. XRF detected contaminant elements such as tantalum and antimony. This may have entered the melt through contaminants in the charge material or contaminated additions, although during testing of additions and charge material none of the above contaminants were detected.

Table 1: X-Ray Fluorescence Testing Results

Fe	Cr	Si	Mn	Mo	Ni	Sn	Sb	Ta	Nb
97.8000	0.8980	0.2600	0.3480	0.2210	0.1070	0.0260	0.0660	0.0860	0.1880

Table 2: Spark Testing Results

C	Cr	Ni	Mo	Si	Mn	Cu	S	P	Al	V	N
0.435	0.97	0.0402	0.164	0.0611	0.353	0.0616	0.0058	0.0146	0.0053	0.0058	0.0127

Of particular note, manganese was below target chemistry for both tests. The lower manganese content seen in both tests suggests it may have been lost due to oxidation during melting; manganese has a large influence on the hardenability of the steel. Manganese delays pearlite and ferrite formation. In steel, hardenability is controlled by the transformation of austenite into other phases, such as martensite, pearlite, or ferrite, during cooling. Manganese is a strong austenite stabilizer meaning it delays the transformation of austenite into ferrite and pearlite; with less manganese ferrite and pearlite form easier during cooling, leaving less time for the martensite transformation. Additionally, manganese increases carbon solubility in austenite, allowing a greater amount of carbon to remain in solution rather than precipitating as carbides. Manganese will also lower the critical cooling rate, meaning that the sword must be quenched faster to maintain a similar hardness. Finally, manganese will slow down diffusion-controlled reactions and increases the depth of hardening. As a result of the low manganese seen, the sword will be softer than it would usually be. Additionally, aluminum is a lower chemistry than the target. Aluminum is used as an alloying element in steel to deoxidize the steel, as oxygen is an undesirable element. Aluminum forms oxide inclusions and brittleness in steel. Aluminum reacts with oxygen to form aluminum oxide, which removes oxygen from liquid metal. The amount of aluminum seen should still serve to deoxidize the steel, although there is an increased risk of oxide inclusions and brittleness.

Interestingly, the data seen for silicon varies much more than other elements between tests. Spark testing measures surface composition while XRF measures bulk composition. The spark test data was much lower than the XRF. If silicon is truly low in the bulk composition there could be higher amounts of oxides in the melt, leading to porosity and reduced toughness. Segregation could also be an issue due to this data. Silicon has a tendency to segregate during cooling, especially in castings. Silicon could have segregated to the last to solidify areas of the mold. This can also occur due to inadequate mixing in the melt. Silicon segregation can have multiple deleterious effects on the quality of the casting. Silicon decreases the surface tension

of the melt, making it easier for gas bubbles to nucleate and grow. Lower surface tension leads to dissolved gas being less likely to remain in solution. In general, it will affect the behavior of mold gases. Silicon also lowers solidification temperature, leading to uneven solidification and shrinkage in silicon rich zones. This would most likely occur in the center and lead to localized shrinkage porosity. Deoxidation may also be uneven if this occurs.

To examine if segregation did occur a Scheil Solidification Simulation was performed with the x-axis representing the fraction of the material that has solidified and the y-axis representing temperature. Elements like silicon and manganese tend to segregate toward the liquid phase in the last to solidify regions. In casting solidification is gradual, so there is a strong chance of segregation. The red line corresponds to ferrite, the green line corresponds to austenite, and the purple line corresponds to an inclusion or segregant region. The non-linear solidification path shows that elements are partitioning into the liquid. In addition to this the late-stage solidification shown on the graph at around 1452°C ensures enrichment of silicon and possibly manganese in the final solidified regions. The gradual slope also indicates a wide freezing range for the alloy; this means that the steel does not solidify uniformly, instead, it goes through a mushy zone where solid and liquid both are present. During this phase, elements like silicon and manganese can segregate to the remaining liquid. This can create hard, brittle zones that are silicon rich. It also increases the chance of shrinkage porosity, as the final liquid regions have issues feeding into the mostly solidified casting and without sufficient feeding, porosity will form. It will also cause issues with gases inside the mold.

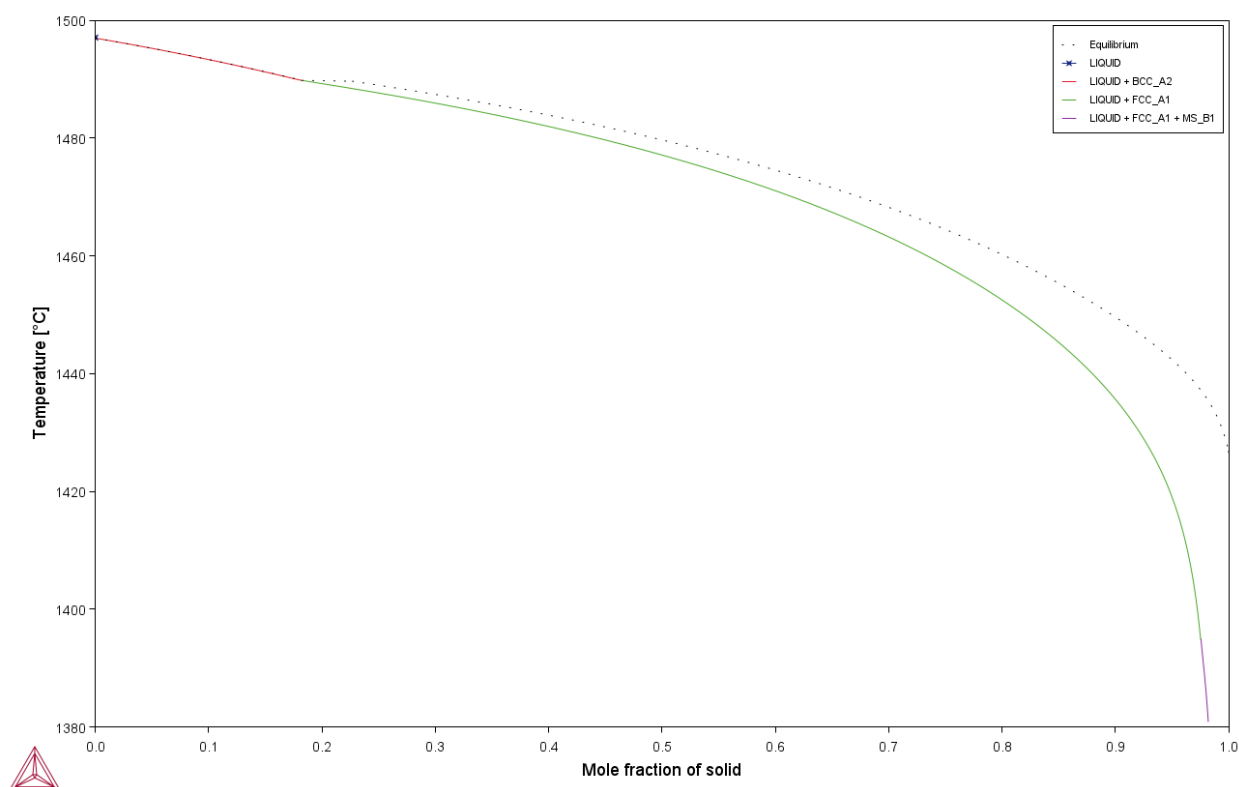


Figure 11: Scheil Solidification Model

After casting the 3 molds and castings were visually inspected for defects. The control exhibited a greater amount of defects than the other 2 castings, with the tang and tip of the sword not casting. It also exhibited significant hot tears, both on the blade and oddly, on the runner. It is clear that the runner needed to be larger to prevent premature freezing, validating the decision to increase the depth of the runner. The second cast sword also exhibited similar hot tears. The hot tears were likely due to the very square shape of the pattern and the large integrated guard, causing the sword to tear with the strong sand and the sword is unable to withstand the tensile stresses induced by shrinkage and thermal contraction. More draft angle and a higher allowance for shrink would have combated this issue. The sword that was cast first had one smaller hot tear on the runner and a small section on the guard that did not cast, but otherwise had no surface defects. It also exhibited a much higher degree of flashing. This sword was cast first, meaning there was a higher superheat upon casting. This is likely the reason for no surface defects due to the melt being at a much higher temperature, allowing more time to fill the mold before solidification began, resulting in a higher quality casting comparative to the others.

Destructive testing was also performed to examine the internal integrity of the blade. Upon cutting open the blade there was significant porosity. Originally it was thought that this was solely due to issues with feeding, but upon testing it was evident that shrinkage porosity due to inadequate feeding was likely a very small part of the issue. Shrinkage porosity was evident across the entire blade, even in spots that the mathematics and metallurgy determine there is zero reason for shrinkage porosity to occur; in essence, there are areas confirmed that no shrinkage porosity can be present with the calculated feeding distance, like in the gates as seen in Figure 12. There was not only porosity in the blade but also right at the gates, which the risers were situated directly next to. Even with inadequate feeding, this region still would have fed correctly and have no porosity. Additionally, when machining off the cast skin, there were significant inclusions seen on the surface that were determined to not be from the mold walls. With the data from spark test and xrf, as well as the subsequent Scheil Solidification Simulation, it seems likely the issue is the melt practice at the Colorado School of Mines facility. This conclusion can also be made because a 4140 casting was manufactured at the Colorado School of Mines foundry, did not exhibit any of the segregation or porosity issues; this casting also had a higher feeding distance than the sword casting. Additionally, test bars and Charpy plates were cast alongside the sword molds and exhibited similar porosity; these molds have been cast in this alloy every year and have never exhibited porosity. Silicon was not added as an addition, instead the silicon content was from the charge material. As a result of this, when it was added to the furnace, it was not controlled. This led to uneven distributions within the melt, and without the proper timing of the addition segregation and silicon oxides formed. The segregation exacerbated the porosity as the uneven regions of silicon likely caused the mushy zone to widen, keeping silicon rich regions liquid longer than the rest of the casting. This led to the risers not feeding long enough and shrinkage porosity forming, even though the feeding seemed sufficient. Although, it could have been inadequate riser volume, it is unlikely due to the above reasons, especially with shrinkage forming so close to the riser.

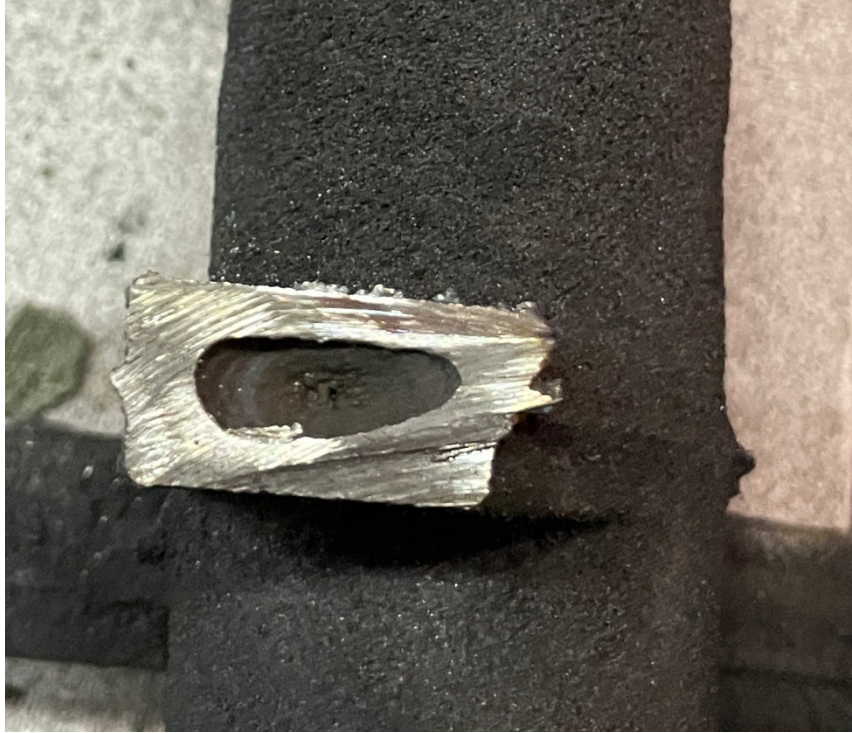


Figure 12: Porosity in Gates

To ensure proper quality of the sword micrographs were also taken. Micrographs were taken for the as-cast, as-forged, and as-tempered conditions, providing data on microstructural evolution throughout post-processing. Micrographs were taken at the same location on the sword to ensure the validity of the data. Small black spots can be seen on all micrographs due to no LECO pads for polishing being available, so old pads had to be utilized. The as-cast condition seen in Figure 13 is characterized by a coarse dendritic structure resulting from solidification in the silica sand mold, indicated by irregular and poorly defined grain boundaries. The casting process led to the formation of primarily equiaxed grains, with some columnar grain formation, with dendritic arms forming due to thermal gradients from solidification. The presence of these dendrites suggests a slow cooling rate, like what is characteristic of sand casting. Furthermore, there is a significant amount of pearlite present, likely proeutectoid pearlite, suggests that the material slowly cooled, and the diffusion-controlled reaction transformed austenite to ferrite and pearlite. The pearlite colonies are coarse, indicating that the steel was poured at a high superheat, and points to the fact that there was sufficient time at high temperature for lamellar spacing growth. Overall, the as-cast microstructure is coarse and non-uniform, with visible dendrites. The mechanical properties in this state are non-optimal for the application due to the coarse pearlitic structure resulting in further processing needed.

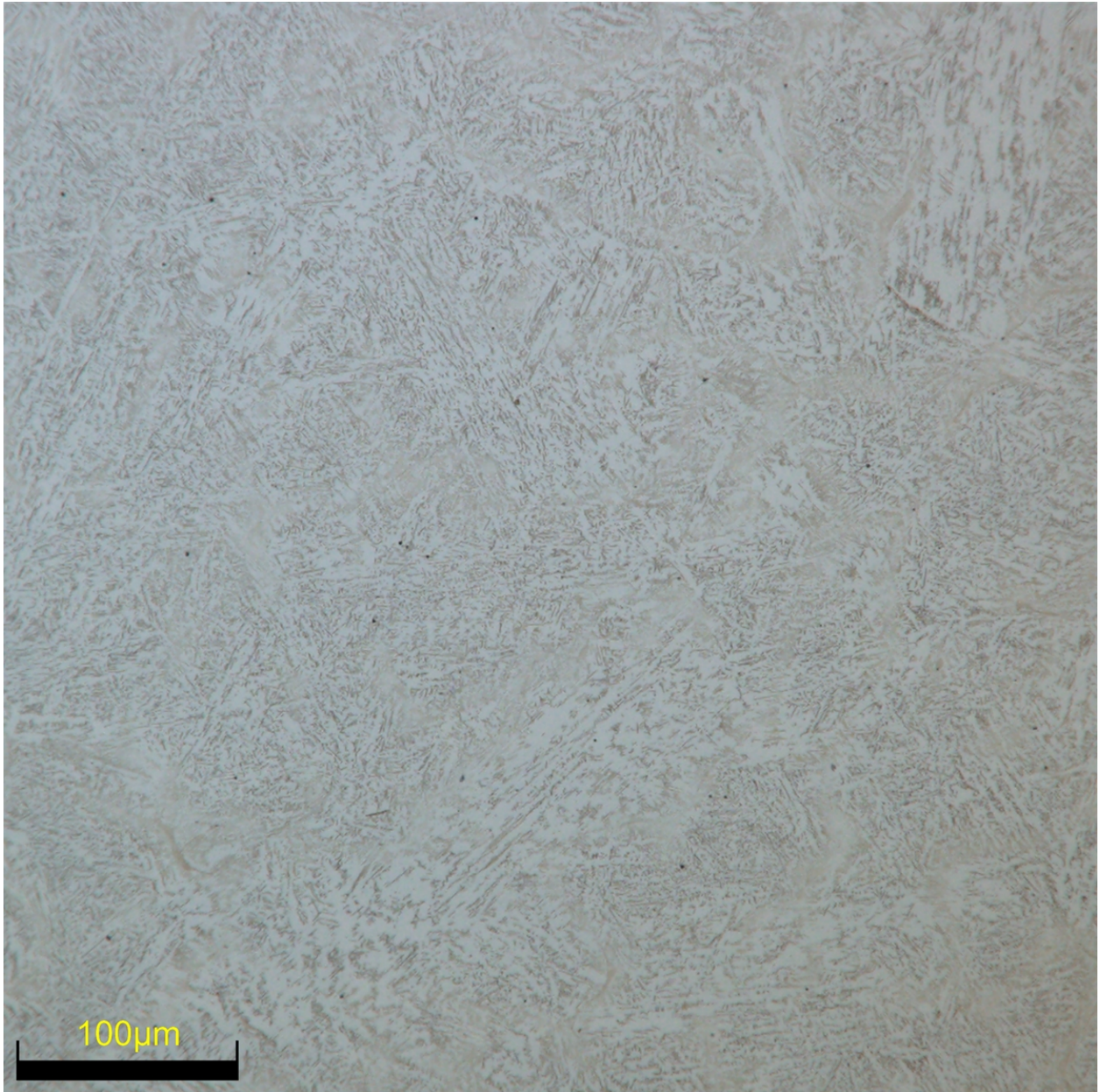


Figure 13: As-Cast Micrograph

Figure 14 showcases the as-forged condition. The dendritic morphology is no longer present, indicating that that forging deformed and recrystallized the grains. A much finer, more uniform, and more equiaxed structure is observed. This indicates that forging deformed the grains, but recovery and recrystallization processes occurred, leading to strain-free, refined grains. One of the largest differences is the pearlite colonies; the microstructure exhibits that the coarse pearlite present in the as-cast condition changes to become finer, and more evenly distributed in the as-forged condition. This microstructure is also more homogeneous, indicating a decrease in segregation effects seen in previous data. Diffusion during the forging process homogenized the composition. Overall, the as-forged microstructure shows a significant improvement over the as-cast state, resulting in finer grains, reduced heterogeneity, and the elimination of the

dendritic structures. This will result in improved mechanical properties, but normalization, austenitizing, and tempering are needed to further improve hardness, toughness, and strength.

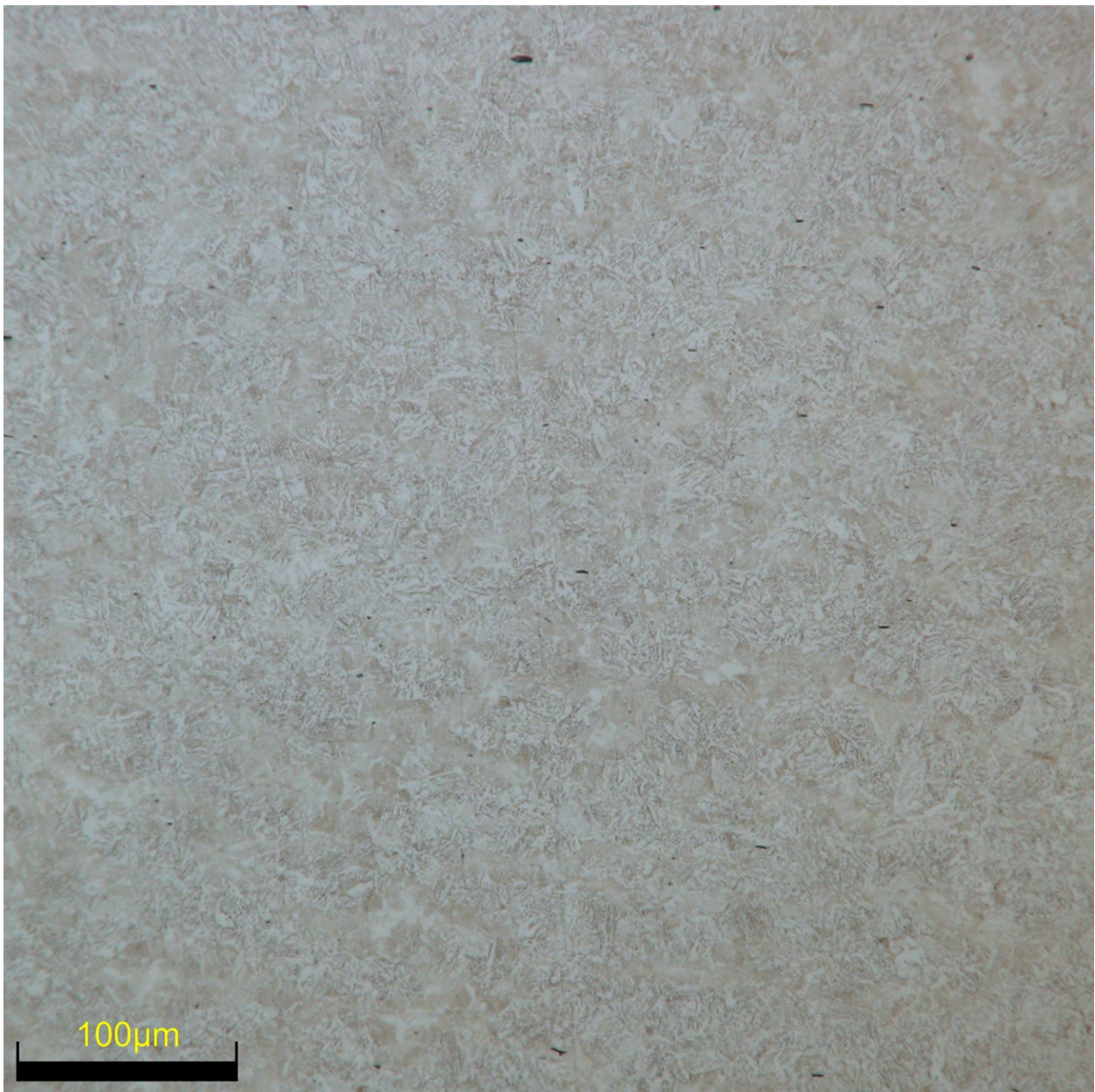


Figure 14: As-Forged Microstructure

Figure 15 shows the microstructure following normalization, austenitizing, and tempering. The microstructure is fully tempered martensite at this stage. Figure 15 is a higher magnification due to the very fine martensite being difficult to view at the previous magnification. The uniformity of the microstructure indicates a complete phase transformation to martensite, and no pearlite colonies or dendrites. Additionally, the uniform appearance of the matrix shows that the tempering process allowed for the redistribution of carbon, resulting in improved ductility in the martensitic phase. Overall, the heat-treated microstructure exhibits a refined and optimal

microstructure for the application, providing the greatest balance in hardness, ductility, and toughness. This microstructure ensures that the sword had the mechanical properties necessary for the demanding application of competition testing.

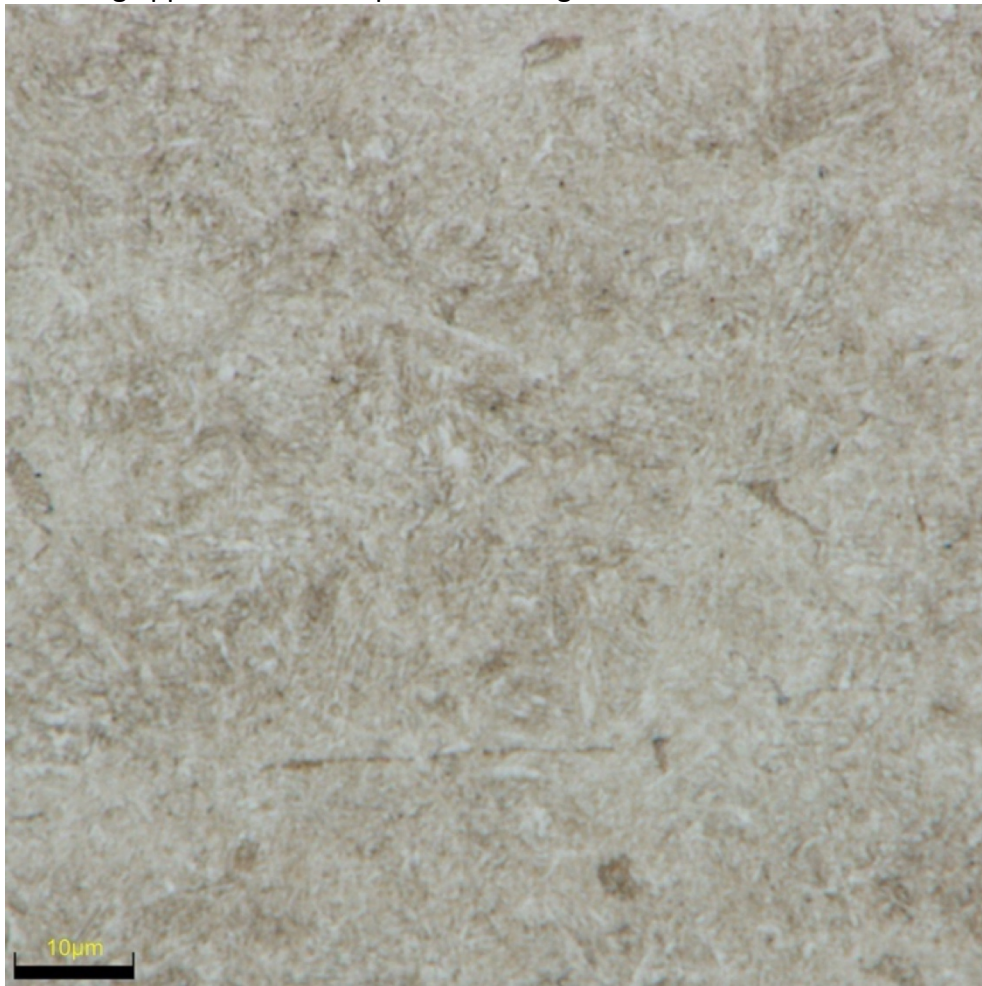


Figure 15: As-Heat Treated Micrograph

Mechanical testing was also completed on the sword, consisting of tensile testing and Hardness Rockwell C testing. These tests were performed according to ASTM E8 and E18, respectively. Test bars for tensile testing were cast from the same heat as the sword according to ASTM 1067. As seen in the other castings, porosity was present in the as-cast condition, so cross-sectional area was calculated as true cross-sectional area, excluding the void. The testing fell outside of the specification for the as-forged and heat treated condition as the gauge lengths were forged to represent the final microstructure of the sword. Additionally, minimal data was able to be taken for the as-forged and as-heat treated condition; the as-forged sample fractured outside the extensometer, so plastic deformation data is minimal, and the as-heat treated condition limited out the load frame. Interestingly, after the load frame limited out the sample fractured despite no increased stress or strain in creep failure. Creep is a time-dependent deformation mechanism that can occur under constant load. Once the sample reached the plastic deformation region, dislocations began to move and accumulate; the sample

continued to deform due to residual stress in the system. This is most likely due to the transition from the forged to the non-forged section of the sample being a stress riser.

Figure 16 shows the stress-strain curves for the tensile samples. All samples fail at relatively low strain due to the porosity in the gauge length. The as-cast condition shows the worst mechanical properties out of all three conditions. It exhibited brittle fracture and had the lowest stiffness, lowest yield point, and lowest ultimate tensile strength. This is due to the high amount of pearlite, the dendritic structure, and larger amount of porosity. The as-forged sample displayed better mechanical properties and a higher stiffness comparative to the other samples. Unfortunately, the sample began to neck outside the extensometer, which is why the curve remains constant in the necking region. Overall, it exhibits a higher toughness, yield point, ultimate tensile strength, and elongation than the as-cast state, validating the decision to forge the blade. This is due to the much finer grain structure, the elimination of the dendritic structure, and the increased phase homogeneity. The as-heat treated condition has the highest higher toughness, yield point, stiffness, and ultimate tensile strength. Unfortunately, the load frame limited out as it entered the plastic region, so mechanical properties are higher than shown. However, it does have a lower ductility. These optimal mechanical properties are due to the very fine martensitic structure present after tempering, making it ideal for the rigorous requirements for testing at competition.

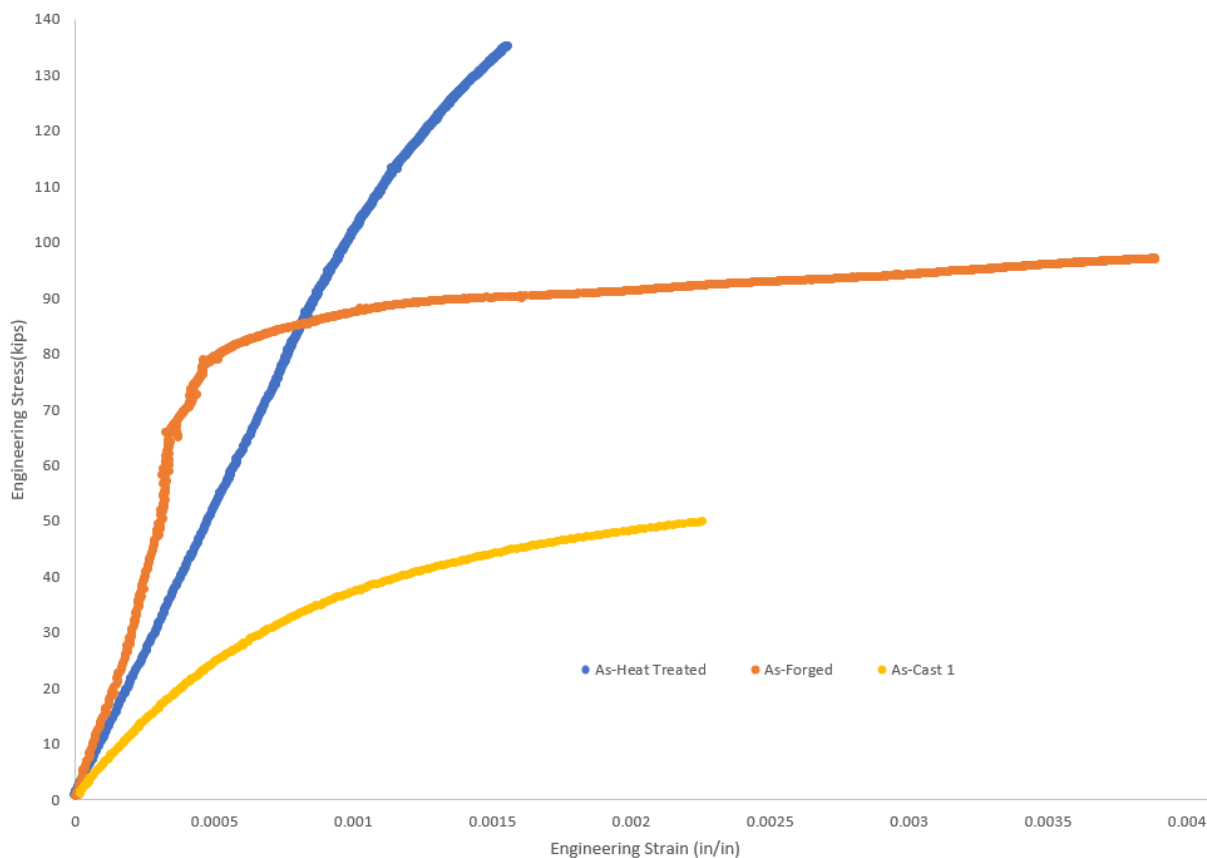


Figure 16: Stress-Strain Curve for the Post-Processing Conditions

Although minimal data was able to be recorded in the stress-strain curves due to how the test bars failed, valuable information was able to be taken from the fracture surfaces and validated by the stress-strain curves. Figure 17, 18, and 19 show the fracture surfaces for the as-cast, as-forged, and as-heat treated conditions. The as-cast condition shows a fracture surface that is jagged, uneven, and shiny, which is indicative of brittle fracture. This may be due to the as-cast microstructure, but more likely that the porosity caused the brittleness as the porosity causes stress concentrations and the cross-section could not support the load into the plastic deformation regime. The as-forged fracture surface exhibits rough, non-shiny characteristics, indicating ductile fracture. The sample exhibited necking during deformation, but occurred outside the extensometer so little data is seen on the plastic deformation of the sample. The as-heat treated sample exhibits similar characteristics of brittle fracture.



Figure 17: As-Cast Test Bar Fracture Surface



Figure 18: As-Forged Test Bar Fracture Surface

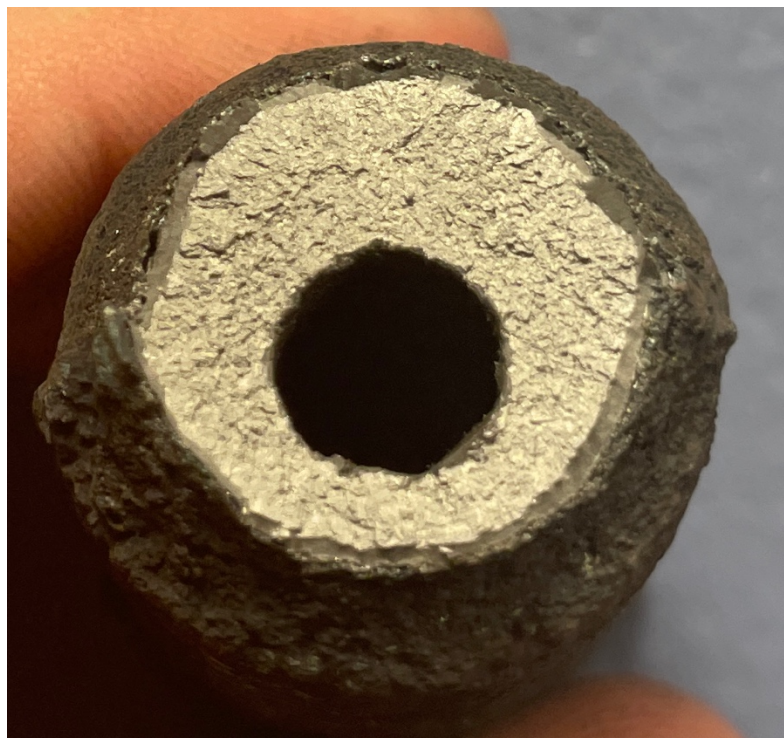


Figure 19: As-Heat Treated Test Bar Fracture Surface

HRC testing was accomplished to characterize the hardness in the different conditions. Tables 5 and 6 showcase the data and HRC value for the overall sample. The first two data points were not considered for the average as those values can vary due to the material settling. Tables 5 and 6 show the data from the experiments for the as-austenitized and quenched, and the as-tempered condition, as these conditions are of the most interest. The as-quenched condition is extremely high, most likely due to the high surface roughness from cast skin and scale that was unable to be removed in its entirety. The as-tempered hardness showcases that the sword will have a greater balance between hardness and ductility, resulting in greater performance during competition settings. While the HRC value is low for a sword, which is typically 60-63 HRC, this gives a greater ductility at the cost of less edge retention.

Table 3: As-Quenched HRC Values

Test Number	HRC
1.	63.9
2.	64.2
3.	65.0
4.	66.8
5.	64.4
Average	65.4

Table 4: As-Tempered HRC Values

Test Number	HRC
1.	57.8
2.	60.1
3.	56.3
4.	54.3
5.	56.7
Average	55.8

Charpy V-Notch testing was originally planned to be done to characterize the toughness and impact resistance of the submission. However, samples were unable to be machined at Colorado School of Mines and the budget was too limited to send the samples to an external source to be machined.

Conclusion:

In conclusion, the Colorado School of Mines submission is an example of a historically accurate cuttöe that George Washington could have used, if not for the detrimental effects of the silicon segregation driven porosity. Despite this challenge, the project successfully demonstrated the capabilities of modern metal casting and foundry metallurgy techniques. The final product is functional and historically accurate steel blade, fit for the first president of the

United States. Beyond the functionality, the submission used symbolic elements, such as the Blaster the Burro pommel and the rouleau triangle handguard, blending modern engineering, bladesmithing techniques, and historical authenticity while still paying tribute to Colorado School of Mines. These additions paid tribute to George Washington's preferences for understated elegance, while also showcasing the different features of investment and sand casting.

While microstructural and melt segregation issues caused porosity to form within the blade, impacting the overall performance, the forging and heat treatment significantly increased the mechanical properties. The change was large enough that the submission can withstand the significant stresses of testing. The post-processing significantly refined the grains and increased the mechanical properties. Additionally, most of the large pores were able to be closed, resulting in fine, distributed porosity. While still not ideal, it is significantly preferable to the as-cast state. The final product shows significant improvements in the phases present, grain refinement, and mechanical properties. The metallurgical and mechanical testing validated the strength and hardness improvements, confirming the potential for the mechanical properties of the cast component.

While the Colorado School of Mines team was proud of the submission, steps need to be taken in the future to improve mechanical properties, quality, and aesthetic of the sword. Ferrosilicon must be added to the ladle, to improve the fluidity and mold filling ability of the melt and to avoid silicon segregation and the deleterious effects associated with it. Additionally, for future submissions investment casting would be the ideal casting method. Cast components like swords are very difficult to cast due to the length and thin cross-sections; in the future, investment casting would result in a higher quality sword, improved mechanical properties, and less excess material. The primary bevel angle was also too thick due to the porosity, meaning that the sword is not as sharp as it optimally should be. As a result, the sword will not perform as well in slicing. In the future, a thinner primary bevel would aid slicing performance. The Colorado School of Mines team is proud to state that the 4140 sword meets contest requirements, with a weight of 2.8 lbs, a blade length of 26.5 in, and an overall length of 34.5 in.

Acknowledgements:

Dr. Gerald Bourne, Associate Department Head of Metallurgical and Materials Engineering, for use of the Colorado School of Mines Physical Metallurgy Laboratory and Bladesmithing Laboratory.

Dr. Stephen Midson, Research Professor of Metallurgical and Materials Engineering, for continued guidance and assistance with foundry metallurgy fundamentals.

Dr. Garrison Hommer, Assistant Research Professor of Mechanical Engineering, for support and assistance with mechanical testing.

Daniel Bourque and Juan Enriquez, Western Foundry, for continued support and assistance with melt practices during the steel pour.

Mason Weems, PhD Student at Colorado School of Mines, for forging assistance and donation of the 1045 steel charge material.

David Rittmeyer, Matthews Additive Technology, for the manufacture of the 3D printed sand molds

William Richardson, for assistance with editing the technical video.

References

[1] Steel Founders Society of America, *Feeding and Riserling Guidelines for Steel Castings*. 2002.

[2] Steel Founders Society of America, *Supplements to Steel Castings Handbook*. 2002.

[2] "Cast in Steel," *Sfsa.org*, 2025. https://www.sfsa.org/subject-areas/castinsteel/#competition_requirements (accessed Mar. 14, 2025).

[3] Asm International. Handbook Committee, *ASM Handbook Volume 15*. Materials Park, Ohio: Asm International, 1990.

[4] Asm International. Handbook Committee, *ASM Handbook Volume 1*. Materials Park, Ohio: Asm International, 1990.

[5] Asm International. Handbook Committee, *ASM Handbook Volume 4*. Materials Park, Ohio: Asm International, 1990.

[6] J. Campbell, *Castings Practice*. Elsevier, 2004.

[7] *Americanrevolutioninstitute.org*, 2024.
<https://www.americanrevolutioninstitute.org/masterpieces-in-detail/american-officers-sword-made-by-john-bailey/>

[8] "George Washington's Mount Vernon," *George Washington's Mount Vernon*, 2024.
<https://www.mountvernon.org/preservation/collections-holdings/washingtons-swords>

[9] E. Goldstein, S. C. Mowbray, B. Hendelson, and Carol Borchert Cadou, *The swords of George Washington*. Woonsocket, Ri: Mowbray Publishing, 2016.

[10] J. H. Schwartz, *Western Pennsylvania History*, vol. 93, "Getting to Know George Washington," 2010